Available online at www.sciencedirect.com
ScienceDirect
Tetrahedron
Tetrahedron 63 (2007) 2829–2839

Inclusion [2]complexes based on the cryptand/diquat recognition motif

Feihe Huang,[a,b,*] Carla Slebodnick,[b] Karen A. Switek[b,†] and Harry W. Gibson[b,*]

[a]*Department of Chemistry, Zhejiang University, Hangzhou 310027, PR China*
[b]*Department of Chemistry, Virginia Polytechnic Institute and State University, Blacksburg, VA 24061, USA*

Received 11 November 2006; revised 20 January 2007; accepted 23 January 2007
Available online 25 January 2007

Abstract—Seven diquat-based inclusion [2]complexes were studied by proton NMR spectroscopy, electrospray ionization mass spectrometry, and X-ray analysis. The hosts used in these inclusion [2]complexes are bis(5-hydroxymethyl-1,3-phenylene)-32-crown-10, a bis(*m*-phenylene)-26-crown-8-based cryptand, and five bis(*m*-phenylene)-32-crown-10-based cryptands. Bis(*m*-phenylene)-32-crown-10-based cryptands have been proved to be able to complex diquat much more strongly than bis(*m*-phenylene)-32-crown-10 itself and one containing a pyridyl moiety has one of the highest K_a values reported to date. These hosts form 1:1 complexes with diquat in solution and in the solid state. It was found that the improved binding from bis(*m*-phenylene)-32-crown-10 to bis(5-hydroxymethyl-1,3-phenylene)-32-crown-10 was due to a supramolecular cryptand structure formed by chelation of the two terminal OH moieties of bis(5-hydroxymethyl-1,3-phenylene)-32-crown-10 with a water molecule as a hydrogen-bonding bridge.

1. Introduction

Inclusion complexes have been widely studied for different purposes.[1] Cryptands, hosts with two points connected by at least three bridges,[2a] are important in the preparation of inclusion complexes. The first cryptand was reported in 1968.[2b] The original objective for preparing cryptands was to bind metal ions and small organic molecules strongly by encapsulation.[2] Recently progress has been made in the synthesis of cryptands and supramolecular cryptands[3] that can complex large organic guests, such as paraquat derivatives,[4] bis(secondary ammonium) salts,[5a] monopyridinium salts,[5b] and tripyridinium salts.[5c] Inspired by the formation of a taco complex in the solid state from paraquat **1** and bis(*m*-phenylene)-32-crown-10 (BMP32C10) derivative **2a**,[4d] in order to prepare large supramolecular systems efficiently from small-building-block-based host–guest chemistry, we designed and prepared a series of crown ether-based cryptands, which can complex paraquat derivatives, such as **1**, much more strongly than the corresponding simple crown ethers.[4d–4h] First we reported very strong complexation between a cryptand and paraquat derivatives in 1999.[4d] Later, we reported cooperative complexation between a cryptand and a bisparaquat derivative,[4e] two pseudorotaxane-like cryptand/paraquat [3]complexes,[4f] and the formation of dimers of cryptand/paraquat inclusion complexes driven by dipole–dipole and face-to-face π-stacking interactions.[4g] Specifically, a bis(*m*-phenylene)-32-crown-10-based diester cryptand with a pyridyl nitrogen atom located at a site occupied by either water or a PF_6 anion in analogous crown ether-based complexes exhibited a very high association constant with paraquat, $K_a=5.0\times10^6\ M^{-1}$ in acetone, 9000 times greater than the crown ether system.[4h] We also found that the formation of supramolecular cryptands by chelation of difunctional macrocycles can improve the complexations with paraquat derivatives,[6a] a bis(secondary ammonium) salt,[5a] and a bisparaquat derivative.[6b] These cryptands and supramolecular cryptands have proven to be much better hosts for organic guests than corresponding simple crown ethers.[4,5a,5b,6] These guest-binding improvements can be ascribed to preorganization[7] and/or multi-point binding.[8] Furthermore, other groups have used cryptands as the hosts to bind inorganic anions,[9] anionic colorimetric dyes,[9] acetic acid,[10] and ion pairs.[11]

Diquat (**3**) is an effective herbicide that presents toxicity challenges to fish, mammals, etc. and thus needs to be carefully monitored in the environment.[12] Partially, for this reason it has been studied as the guest in numerous inclusion complexes.[13] Paraquat derivatives (viologens) are *N*,*N*′-dialkyl-4,4′-bipyridinium salts and some of them are also effective herbicides, while diquat is a 2,2′-bipyridinium salt. Both paraquat derivatives and diquat have two charges and two electron-poor pyridinium rings. Just like the PF_6 salt

Keywords: Host–guest systems; Self-assembly; Complex; Cryptand; Diquat.
* Corresponding authors. Tel./fax: +86 571 8795 3189 (F.H.); tel.: +1 540 231 5902; fax: +1 540 231 8517 (H.W.G.); e-mail addresses: fhuang@zju.edu.cn; hwgibson@vt.edu
† Summer Undergraduate Research Participant, 1999, supported by the National Science Foundation through DMR 922487 REU. Present address: Department of Chemistry, University of Minnesota, Minneapolis, MN 55455-0431, USA.

0040–4020/$ - see front matter © 2007 Elsevier Ltd. All rights reserved.
doi:10.1016/j.tet.2007.01.042

of paraquat, the PF_6 salt of diquat is also a white solid. Since bis(*m*-phenylene)-32-crown-10 (BMP32C10, **2b**) and diquat also form a complex,[13e] we reasoned that BMP32C10-based cryptands should also be able to complex diquat even more strongly. Here we demonstrate that this is true by the study of complexation between five cryptands (**4a**,[4d] **4b**,[4h] **4c**,[4h] **4d**,[4h] and **4e**[4h]) and diquat **3**. In order to determine how the crypt- and ring size affects the binding of diquat, the complexation between a bis(*m*-phenylene)-26-crown-8-based cryptand[4f] (**5**) and diquat **3** was also studied. Furthermore, we found that BMP32C10 diol **2a** can bind diquat **3** stronger than BMP32C10 (**2b**) itself due to the formation of a supramolecular cryptand structure formed by chelating the terminal OH moieties of **2a** with a water molecule as a hydrogen-bonding bridge.

2. Results and discussion

2.1. Proton NMR study of complexation of cryptands 4 and 5 and crown ether 2a with diquat 3

Equimolar (1.00 mM) acetone solutions of each of the cryptands **4** and **5** and the crown ether **2a** with diquat **3** were yellow due to charge transfer between the electron-rich aromatic rings of the cryptand or crown ether host and the electron-poor pyridinium rings of the guest **3**. Job plots[14] (Fig. 1) based on proton NMR data demonstrated that all seven complexes were of 1:1 stoichiometry in solution.

Only one set of peaks was found in the proton NMR spectra of the solutions of each of cryptands **4** and **5** and crown ether **2a** with diquat **3**, indicating that all seven host–guest complexes are fast-exchange systems. As an example, partial proton NMR spectra of **4a**, **3**, and a mixture of **4a** and **3** are shown in Figure 2. Significant upfield shifts of aromatic protons H_1 and α-ethyleneoxy protons H_2 on **4a** and *N*-methylene protons H_6 of **3** and a downfield shift of β-ethyleneoxy protons H_3 on **4a** are observed. The association constant (K_a) of **4a**·**3** calculated based on the proton NMR data was 4.3 (±0.4)×10^4 M^{-1} in acetone-d_6,[15] which is a little lower than the K_a of **4a**·**1**, 6.1×10^4 M^{-1} in acetone-d_6,[4d] but about 110 times higher than the K_a of **2b**·**3**, 390 M^{-1} in acetone-d_6.[13e] The association constants for complexes **4c**·**3**, **4d**·**3**, **4e**·**3**, **5**·**3**, and **2a**·**3** were determined in the same way as that of **4a**·**3**.[15] K_a values for all seven complexes are summarized in Table 1 with the previously reported K_a value for **2b**·**3**. Compared with the K_a value of **2b**·**3**, the complex based on the simple crown ether, K_a values of cryptand complexes **4c**·**3**, **4d**·**3**, and **4e**·**3** increased about 18-, 3.4-, and 1.4-fold, respectively.

The K_a of **4b**·**3** was determined using a competitive method developed by the Smith Group[17] to be 3.3 (±0.7)×10^5 M^{-1} in acetone-d_6,[18] which is lower than the K_a of **4b**·**1**, 5.0 (±2.0)×10^6 M^{-1} in acetone-d_6,[4h] but about 360 times higher than K_a of **2b**·**3**. Thus it was demonstrated that BMP32C10-based cryptands **4** are able to complex diquat **3** much more strongly than the corresponding simple crown ether, BMP32C10 (**2b**). In comparison, a porphyrin-linked bis(*m*-phenylene)-32-crown-10-based cryptand bound **3** with K_a=1.2×10^5 M^{-1} (CD_3COCD_3/$CDCl_3$, 86:14).[13j] Dibenzo-30-crown-10 is reported to bind diquat **3** with K_a=1.75×10^4 M^{-1} (CD_3COCD_3),[13a] while a dibenzo-30-crown-10-based cryptand exhibited K_a=2.6×10^5 M^{-1} (CD_3COCD_3).[13d]

Similar to paraquat complexes reported recently,[4h] the improvement from crown ether complex **2b**·**3** to cryptand complexes **4d**·**3** and **4e**·**3** can be mainly attributed to

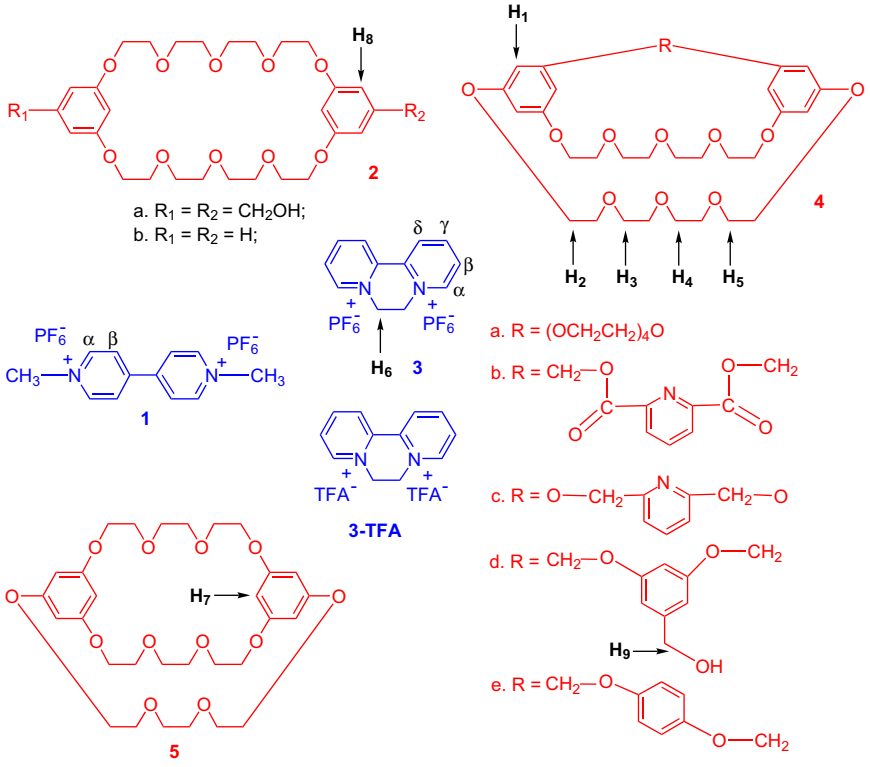

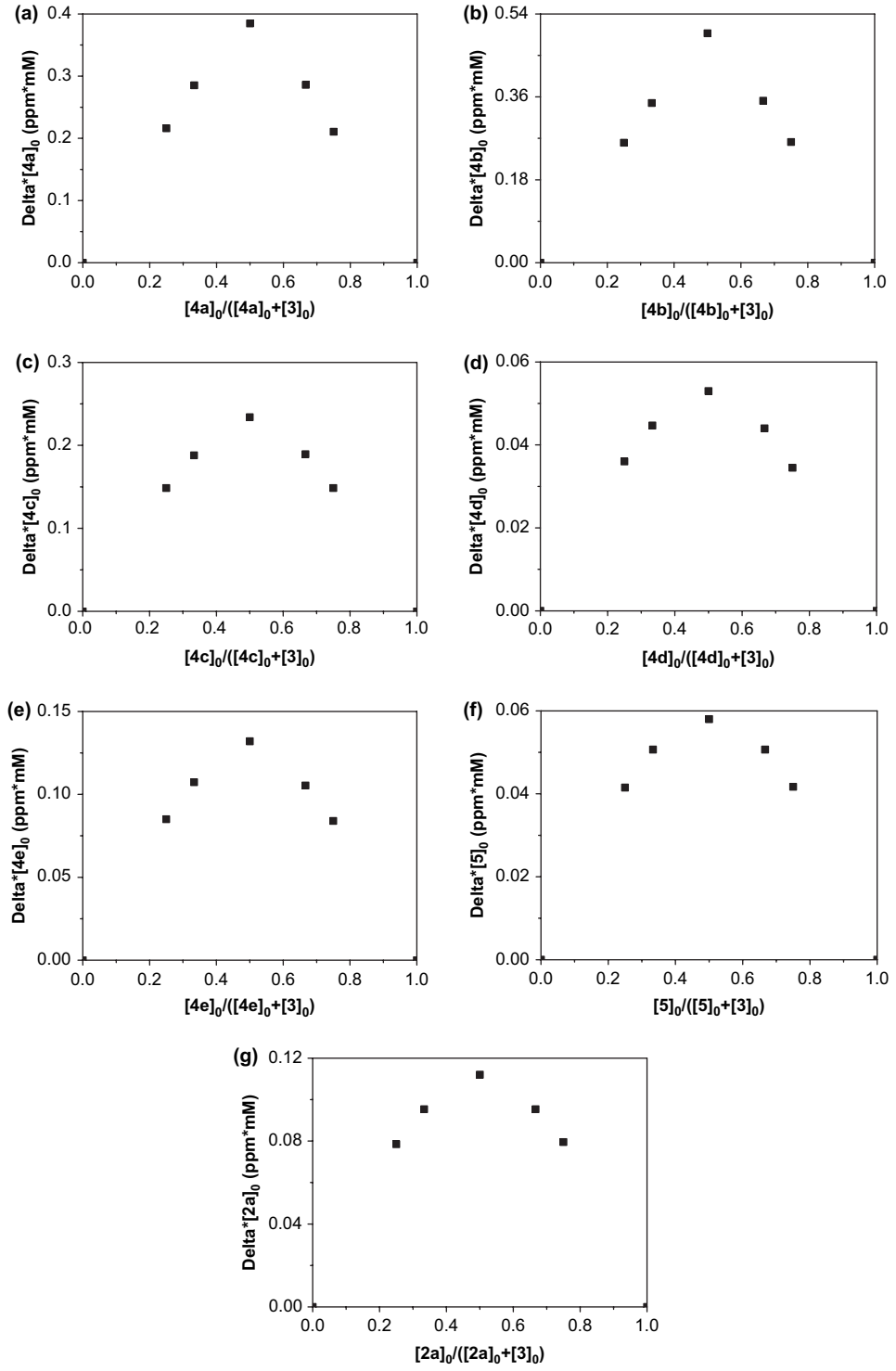

Figure 1. Job plots showing the 1:1 stoichiometries of the complexes between **4a** and **3** (a), between **4b** and **3** (b), between **4c** and **3** (c), between **4d** and **3** (d), between **4e** and **3** (e), between **5** and **3** (f), and between **2a** and **3** (g) in CD_3COCD_3. For all solutions, the sum of initial concentrations of the cryptand or crown ether host and diquat guest was 2.00 mM. Delta=chemical shift change for H_1 of **4a**, **4b**, **4c**, and **4e**, H_9 of **4d**, H_7 of **5**, and H_8 of **2a**.

the preorganization of the cryptand hosts, while the improvement from **4d**·**3** to **4c**·**3** is due to the introduction of an additional binding site, the pyridyl nitrogen atom. The great increase in association constant from crown ether complex **2b**·**3** to pyridyl ester cryptand complex **4b**·**3** is a result of the combination of the preorganization of the host and the introduction of an additional binding site. The K_a (6.1×10^4 M^{-1}) of cryptand/paraquat complex **4a**·**1**[4d] is about four times the K_a (1.4×10^4 M^{-1}) of smaller cryptand/paraquat complex **5**·**1**,[4f] while the K_a (4.3×10^4 M^{-1}) of cryptand/diquat complex **4a**·**3** is about 83 times the K_a (5.2×10^2 M^{-1}) of smaller cryptand/paraquat complex **5**·**3**. This indicates that the size of the cryptand host has a much more important influence on the binding ability of the dicationic guest diquat (**3**) because it is wider than paraquat **1**. CH_2OH has a Hammett σ value of zero[19] and thus is

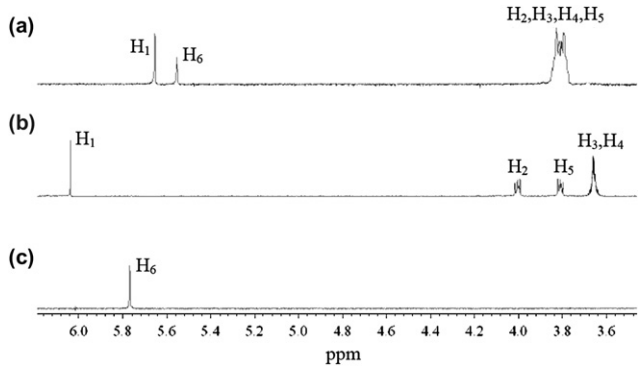

Figure 2. Partial proton NMR spectra (400 MHz, acetone-d_6, 22 °C) of 1.00 mM **3** and 1.00 mM **4a** (a, top), cryptand **4a** (b, middle), and diquat **3** (c, bottom).

not expected to influence the complexation of **2a** with **3** electronically. Therefore the 6-fold increase in association constant from unsubstituted crown ether complex **2b**·**3** to crown ether diol **2a**·**3** is presumably due to the formation of a supramolecular cryptand structure with the latter, as observed in crystal structures of both **2a**·**3** and **2a**·**3**-TFA (see below).

2.2. Solid-state structure of diquat 3

A single crystal of guest **3** for X-ray analysis was grown by vapor diffusion of pentane into an acetone solution. As shown by its crystal structure (Fig. 3), the two pyridinium rings of **3** are twisted at an angle of 18.5° and a centroid–centroid distance of 4.23 Å.

2.3. Solid-state structure of cryptand/diquat [2]complex 4a·3

The formation of the inclusion complex **4a**·**3** was confirmed by X-ray analysis (Fig. 4). X-ray quality, yellow single crystals of **4a**·**3** were grown by vapor diffusion of pentane into an acetone solution of **3** with excess **4a**. When crystals of diquat-based complexes mentioned in this paper were treated with solvents, we found that they were insoluble in pentane, hexane, and ethyl ether, but soluble in acetone and acetonitrile. The 1:1 complex **4a**·**3** is stabilized by hydrogen bonding and face-to-face π-stacking interactions in the solid state. Three *N*-methylene hydrogens (**A**, **B**, and **E** in Fig. 4), one α-pyridinium hydrogen (**C** and **D** in Fig. 4), and one β-pyridinium hydrogen (**I** in Fig. 4) are directly hydrogen bonded to ethyleneoxy oxygen atoms of the host. One δ-pyridinium hydrogen is indirectly connected to an ethyleneoxy chain of host **4a** by a hydrogen-bonding water bridge (**F**, **G**, and **H** in Fig. 4). This is interesting since the two β-pyridinium hydrogens of paraquat (**1**) are also connected to an ethyleneoxy chain of cryptand host **4a** by a hydrogen-bonding water bridge in the 1:1 complex **4a**·**1**.[4d] Furthermore, neither of the δ-pyridinium hydrogens

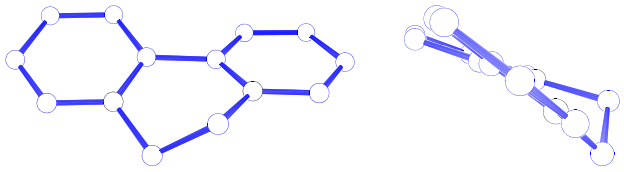

Figure 3. Two ball-stick views of the solid-state structure of diquat (**3**) as determined by X-ray crystallography. The PF_6 counterions and hydrogens have been omitted for clarity. The angle and centroid–centroid distance between two pyridinium rings of **3** (deg and Å): 18.5 and 4.23.

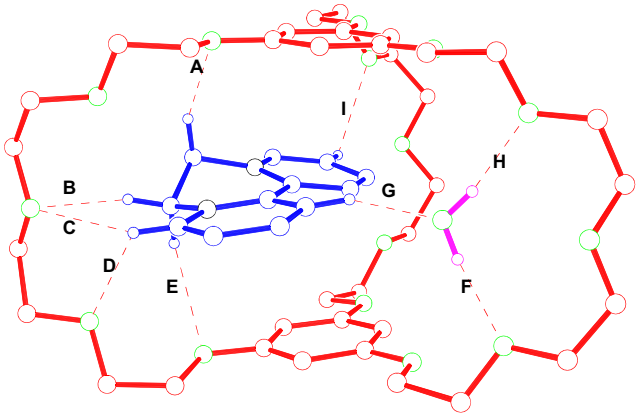

Figure 4. A ball-stick view of the X-ray structure of cryptand/diquat complex **4a**·**3**. **4a** is red, **3** is blue, the water molecule is magenta, oxygens are green, and nitrogens are black. Two PF_6 counterions, other solvent molecules, and hydrogens except the ones involved in hydrogen bonding between **4a** and **3** were omitted for clarity. Hydrogen-bond parameters: H···O distances (Å), C(O)–H···O angles (deg), C(O)···O distances (Å) **A**, 2.47, 153, 3.38; **B**, 2.29, 162, 3.25; **C**, 2.60, 146, 3.43; **D**, 2.65, 119, 3.21; **E**, 2.65, 134, 3.42; **F**, 1.99, 173, 2.85; **G**, 2.27, 137, 3.04; **H**, 1.98, 170, 2.84; **I**, 2.77, 124, 3.40. Face-to-face π-stacking parameters: centroid–centroid distances (Å) 3.72, 4.09, 4.05, 4.68; ring plane/ring plane inclinations (deg): 7.4, 1.6, 14.0, 8.4. The centroid–centroid distance (Å) and dihedral angle (deg) between two phenylene rings of **4a**: 6.79 and 6.8. The centroid–centroid distance (Å) and dihedral angle (deg) between the pyridinium rings of **3**: 4.23 and 15.5.

is involved in interactions between the host and guest in the 1:1 crown ether/diquat complex **2b**·**3**.[13e] Neither of the γ-pyridinium hydrogens of **3** is involved in hydrogen bonding to the cryptand host in **4a**·**3**, but one γ-pyridinium carbon has a short contact with an ethyleneoxy oxygen atom of **2b** in the 1:1 complex **2b**·**3** based on the simple crown ether.[13e]

The values of the dihedral angle between the two pyridinium rings of **3** in uncomplexed **3**, **2b**·**3**, and **4a**·**3** are 18.5° (Fig. 3), 20°,[13e] and 15.5° (Fig. 4), respectively. The two aromatic rings of the cryptand host in **4a**·**3** are almost parallel (6.8°) with a centroid–centroid distance of 6.79 Å, a value smaller than the corresponding values, 6.94 Å in the corresponding paraquat complex **4a**·**1**,[4d] and 7.0 Å in the crown ether complex **2b**·**3**, whose crystals are yellow.[13e] These

Table 1. Association constants for complexes of diquat **3** with crown ethers **2a** and **2b** and different cryptands **4** and **5** in 1 mM host and guest acetone-d_6 solutions at 22 °C[15]

	2b·**3**	**4a**·**3**	**4b**·**3**	**4c**·**3**	**4d**·**3**	**4e**·**3**	**5**·**3**	**2a**·**3**
$K_a\times10^{-3}$ (M^{-1})	0.39[a]	43 (±4)	3.3 (±0.7)×10^2	7.4 (±0.7)	1.7 (±0.2)	0.93 (±0.09)	0.52 (±0.05)	2.8 (±0.3)

[a] K_a of complex **2b**·**3** was reported before.[13e]

rotational changes take place presumably in order to maximize face-to-face π-stacking and charge transfer interactions between the two electron-rich phenylene rings of the cryptand host and the two electron-poor pyridinium rings of the diquat guest, leading to the bright yellow color of crystals of **4a**·**3**.

2.4. Solid-state structure of cryptand/diquat [2]complex 5·3

The 1:1 stoichiometry of complexation between **5** and **3** in solution was confirmed by X-ray analysis (Fig. 5). X-ray quality, yellow single crystals of **5**·**3** were grown by vapor diffusion of pentane into an acetone solution of **3** with excess **5**. The asymmetric unit of the crystal structure comprises two **5**·**3** complexes. They are connected by two hydrogen bonds (**Q** and **R**). Both of them are stabilized by hydrogen bonding and face-to-face π-stacking interactions in the solid state as in the homologous cryptand/diquat complex **4a**·**3**. The number of hydrogen bonds between **5** and **3** and the involved hydrogens, carbons, and oxygens are the same for the two **5**·**3** complexes, while the hydrogen-bonding parameters have small differences. For both **5**·**3** complexes, one *N*-methylene hydrogen (**O**, **N**, **O1**, and **N1**), one α-pyridinium hydrogen (**P** and **P1**), and two δ-pyridinium hydrogens (**J**, **K**, **L**, **M**, **J1**, **K1**, **L1**, and **M1**) are hydrogen bonded to ethyleneoxy oxygen atoms of host **5**. Neither of β-pyridinium hydrogens of **3** is hydrogen bonded to ethyleneoxy oxygen atoms of host **5** in these **5**·**3** complexes, while one β-pyridinium hydrogen of **3** is hydrogen bonded to ethyleneoxy oxygen atoms of the larger cryptand host **4a** in **4a**·**3** (**I** in Fig. 4). As in the crystal structure of **4a**·**3**, neither of the γ-pyridinium hydrogens is involved in interactions between the host and guest in **5**·**3**. One δ-pyridinium hydrogen of **3** is indirectly connected to one ethylene glycol chain of the larger cryptand host **4a** in **4a**·**3** (Fig. 4), while the two δ-pyridinium hydrogens of **3** are directly connected to an ethylene glycol chain of the small cryptand host **5** by four hydrogen bonds in the two **5**·**3** complexes (Fig. 5).

The values of the dihedral angle between the two pyridinium rings of **3** in the two **5**·**3** complexes are 19.8° and 18.3°,

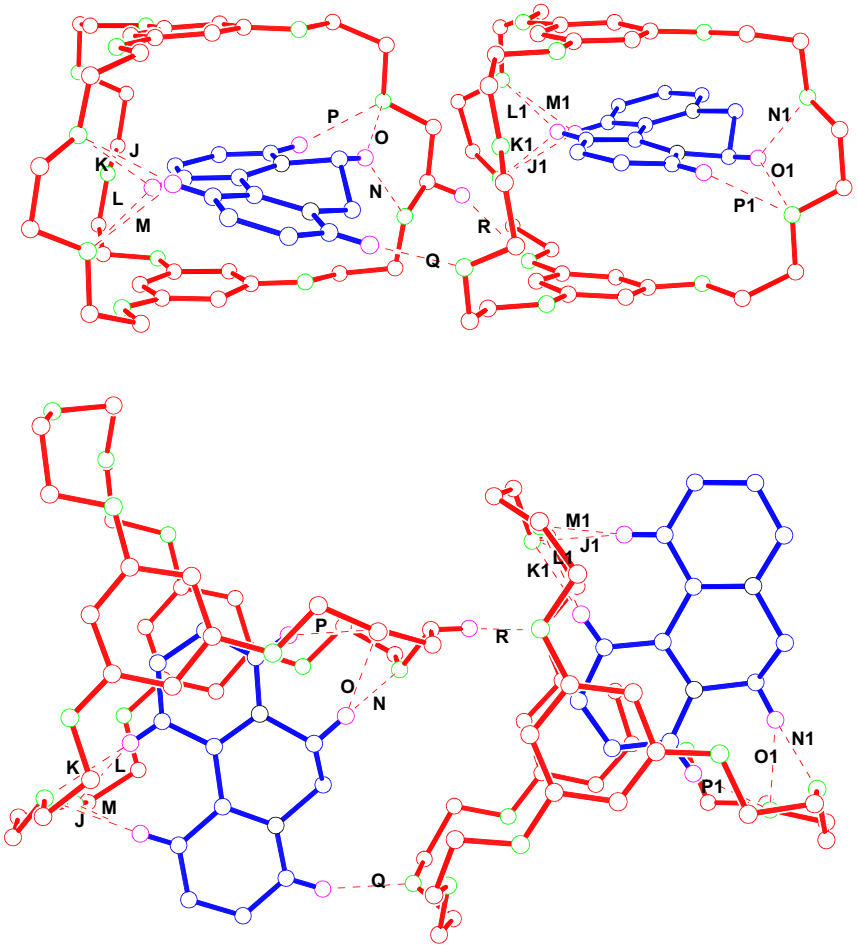

Figure 5. Two ball-stick views of the X-ray structure of cryptand/diquat complex **5**·**3**. **5** is red, **3** is blue, hydrogens are magenta, oxygens are green, and nitrogens are black. Four PF_6 counterions, solvent molecules, and hydrogens except the ones involved in hydrogen bonding between **5** and **3** and between two complexes were omitted for clarity. Hydrogen-bond parameters: H···O distances (Å), C–H···O angles (deg), C···O distances (Å) **J**, 2.54, 139, 3.32; **K**, 2.46, 170, 3.40; **L**, 2.52, 125, 3.16; **M**, 2.51, 157, 3.40; **N**, 2.30, 139, 3.11; **O**, 2.46, 139, 3.27; **P**, 2.40, 146, 3.23; **Q**, 2.26, 160, 3.17; **R**, 2.51, 158, 3.45; **J1**, 2.55, 137, 3.31; **K1**, 2.42, 166, 3.35; **L1**, 2.49, 128, 3.16; **M1**, 2.51, 158, 3.41; **N1**, 2.35, 139, 3.16; **O1**, 2.47, 140, 3.29; **P1**, 2.36, 149, 3.21. Face-to-face π-stacking parameters: centroid–centroid distances (Å) 3.57 and 3.44 for the left complex, 3.47 and 3.54 for the right complex; ring plane/ring plane inclinations (deg): 3.9 and 4.5 for the left complex, 5.7 and 5.6 for the right complex. The centroid–centroid distance (Å) and dihedral angle (deg) between two phenylene rings of **5**: 6.32 and 5.3 for the left complex and 6.28 and 6.7 for the right complex. The centroid–centroid distance (Å) and dihedral angle (deg) between the pyridinium rings of **3**: 4.22 and 19.8 for the left complex and 4.23 and 18.3 for the right complex.

close to the corresponding value, 18.5°, in uncomplexed **3** (Fig. 3), but not so close to the corresponding value, 15.5°, in the larger cryptand complex **4a**·**3** (Fig. 4). The two aromatic rings of the host in the two **5**·**3** complexes are almost parallel (5.3° and 6.7°) with centroid–centroid distances of 6.32 Å and 6.28 Å, values smaller than the corresponding values, 6.81 Å in corresponding paraquat [3]complex **5**·**1**·**5**,[4e] and 6.79 Å in the larger cryptand complex **4a**·**3**. These shorter distances presumably result from maximization of face-to-face π-stacking and charge transfer interactions between the two electron-rich phenylene rings of the cryptand host and the two electron-poor pyridinium rings of the diquat guest, leading to the bright yellow color of crystals of **5**·**3**. In both complexes, only one electron-poor pyridinium ring of **3** has face-to-face π-stacking and charge transfer interactions with the electron-rich phenylene rings of the cryptand host (Fig. 5), while both pyridinium rings of **3** have these interactions with the larger cryptand host in **4a**·**3** (Fig. 4).

2.5. Solid-state structures of crown ether diol/diquat [2]complexes 2a·3 and 2a·3-TFA

The formation of the inclusion complex **2a**·**3** was also confirmed by X-ray analysis (Fig. 6) of an X-ray quality orange single crystal grown by vapor diffusion of pentane into an acetone solution of **3** with excess **2a**. Surprisingly, the asymmetric unit of the crystal structure comprises 1.5 crown ether molecules **2a**, 1 diquat (**3**) molecule, 0.5 acetone molecule, and 1.5 water molecules. Therefore, there is not only a **2a**·**3** host/guest complex, but also an uncomplexed **2a** molecule with 50% occupancy in the crystal structure (Fig. 6). A disordered acetone molecule was found in the cavity of the uncomplexed crown ether molecule. The 1:1 complex **2a**·**3** is also stabilized by hydrogen bonding and face-to-face π-stacking interactions in the solid state are as the above cryptand/diquat complexes **4a**·**3** and **5**·**3**. Two *N*-methylene hydrogens (**V** and **W** in Fig. 6) are directly hydrogen bonded to ethyleneoxy oxygen atoms of host **2a**. One δ-pyridinium hydrogen is indirectly connected to two terminal alcohol groups of host **2a** by a hydrogen-bonding water bridge (**S**, **T**, and **U** in Fig. 6) to form a supramolecular cryptand structure similar to what we observed in the reported complex between **2a** and a bis(secondary ammonium) salt.[5a] The formation of this supramolecular cryptand structure presumably resulted in the 6-fold increase in association constant from **2b**·**3** to **2a**·**3** (Table 1); the same phenomenon was observed when the guest was a bis(secondary ammonium) salt.[5a] None of α-, β-, and γ-pyridinium hydrogens of **3** is involved in interactions between the host and guest in complex **2a**·**3** in the solid state.

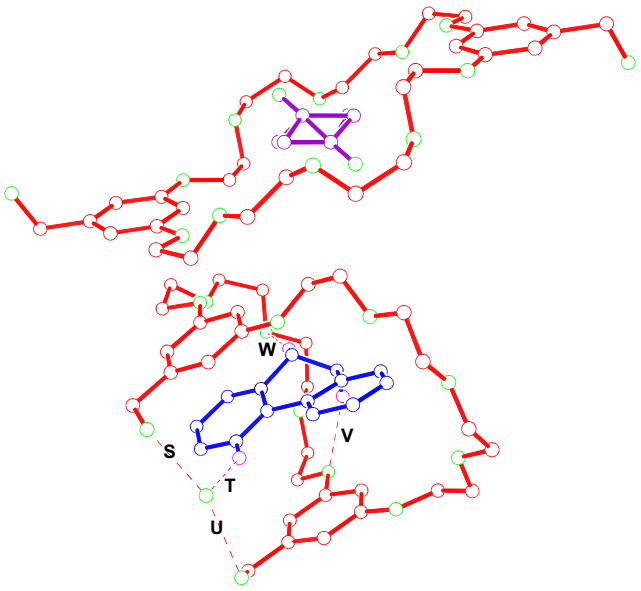

Figure 6. A ball-stick view of the X-ray structure of a single crystal grown by vapor diffusion of pentane into an acetone solution of diquat (**3**) with excess crown ether diol **2a**. **2a** is red, **3** is blue, the disordered acetone molecule is purple, hydrogens are magenta, oxygens are green, and nitrogens are black. Two PF_6 counterions, other solvent molecules, and hydrogens except the ones involved in hydrogen bonding between **2a** and **3** were omitted for clarity. Hydrogen-bond parameters: H···O distances (Å), C(O)–H···O angles (deg), C(O)···O distances (Å) **S**, NA (not available), NA, 2.72; **T**, 2.34, 150, 3.19; **U**, NA, NA, 2.73; **V**, 2.51, 152, 3.41; **W**, 2.48, 167, 3.45. Face-to-face π-stacking parameters: centroid–centroid distances (Å) 4.16, 3.77, 4.07, 4.49; ring plane/ring plane inclinations (deg): 10.5, 3.0, 6.3, 13.8. The centroid–centroid distance (Å) and dihedral angle (deg) between the phenylene rings of **2a**: 6.67 and 7.5. The centroid–centroid distance (Å) and dihedral angle (deg) between the pyridinium rings of **3**: 4.22 and 16.7.

Here the value of the dihedral angle between the two pyridinium rings of **3** in **2a**·**3** is 16.7° (Fig. 6), close to the corresponding value, 15.5°, in cryptand/diquat complex **4a**·**3**, but not so close to the corresponding value, 18.5°, in the uncomplexed **3** (Fig. 3). The two aromatic rings of the host in **2a**·**3** are also almost parallel (7.5°) with a centroid–centroid distance of 6.67 Å (Fig. 6), a value bigger than the corresponding values, 6.32 Å and 6.28 Å in small cryptand/diquat complex **5**·**3** and smaller than the corresponding values, 7.39 Å in the corresponding paraquat complex **2a**·**1**,[4d] 6.79 Å in large cryptand/diquat complex **4a**·**3**, and 7.0 Å in crown ether/diquat complex **2b**·**3**.[13e]

The formation of the supramolecular cryptand structure by chelating two terminal OH moieties of **2a** by a water hydrogen-bonding bridge was further confirmed by X-ray analysis (Fig. 7) of a single crystal of **2a**·**3-TFA** grown by vapor diffusion of pentane into an acetone solution of **3** with excess **2a** and tetraethylammonium trifluoroacetate. In this crystal structure, no uncomplexed crown ether **2a** was found. As in **2a**·**3** (Fig. 6) and cryptand/diquat complexes **4a**·**3** (Fig. 4) and **5**·**3** (Fig. 5), the 1:1 complex **2a**·**3-TFA** is also stabilized by hydrogen bonding and face-to-face π-stacking interactions in the solid state. Three *N*-methylene hydrogens (**Y**, **A1**, and **G1** in Fig. 7), one α-pyridinium hydrogen (**X** and **Z**), and one β-pyridinium hydrogen (**F1**) are directly hydrogen bonded to ethyleneoxy oxygen atoms of host **2a**. Two δ-pyridinium hydrogens are indirectly connected to two terminal alcohol groups of host **2a** by a hydrogen-bonding water bridge (**B1**, **C1**, **D1**, and **E1**) to form the same kind of supramolecular cryptand structure as observed in **2a**·**3**. This further demonstrates that the water-chelated supramolecular cryptand structure can form when crown ether host **2a** complexes diquat guest **3**. Here the chelation is formed presumably in order to maximize face-to-face π-stacking and charge transfer interactions and provide an additional hydrogen-bonding stabilizing force between the crown ether host and diquat guest. As in the above-mentioned cryptand/diquat complexes **4a**·**3** (Fig. 4) and **5**·**3** (Fig. 5) and crown ether diol/diquat complex **2a**·**3**

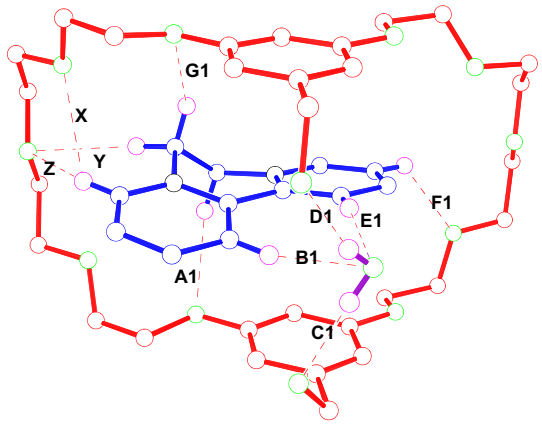

Figure 7. A ball-stick view of the X-ray structure of crown ether diol/diquat complex **2a**·**3-TFA**. **2a** is red, **3** is blue, the water molecule is purple, hydrogens are magenta, oxygens are green, and nitrogens are black. Two trifluoroacetate counterions, other solvent molecules, and hydrogens except the ones involved in hydrogen bonding between **2a** and **3-TFA** were omitted for clarity. Hydrogen-bond parameters: H···O distances (Å), C(O)–H···O angles (deg), C(O)···O distances (Å) **X**, 2.62, 121, 3.22; **Y**, 2.53, 160, 3.48; **Z**, 2.59, 151, 3.45; **A1**, 2.52, 147, 3.39; **B1**, 2.45, 162, 3.37; **C1**, 2.00, 167, 2.84; **D1**, 2.00, 166, 2.81; **E1**, 2.46, 167, 3.39; **F1**, 2.59, 131, 3.29; **G1**, 2.63, 132, 3.37. Face-to-face π-stacking parameters: centroid–centroid distances (Å) 4.40, 4.31, 3.76, 4.52; ring plane/ring plane inclinations (deg): 8.3, 8.9, 10.5, 9.8. The centroid–centroid distance (Å) and dihedral angle (deg) between the phenylene rings of **2a**: 6.98 and 1.2. The centroid–centroid distance (Å) and dihedral angle (deg) between the pyridinium rings of **3**: 4.23 and 18.7.

(Fig. 6), none of the γ-pyridinium hydrogens of **3** is involved in interactions between the host and guest in the complex **2a**·**3-TFA** in the solid state (Fig. 7).

The value of the dihedral angle between the two pyridinium rings of **3** in **2a**·**3-TFA** is 18.7° (Fig. 7), very close to the corresponding value, 18.5° in the uncomplexed **3** (Fig. 3), but not so close to the corresponding value, 16.7° in **2a**·**3**. The two aromatic rings of the host in **2a**·**3-TFA** are also almost parallel (1.2° inclination) with a centroid–centroid distance of 6.98 Å (Fig. 7), a value very close to the corresponding value, 7.0 Å, in **2b**·**3**,[13e] and bigger than the corresponding values, 6.79 Å in large cryptand/diquat complex **4a**·**3**, 6.32 Å and 6.28 Å in small cryptand/diquat complex **5**·**3**, and 6.67 Å in crown ether diol/diquat complex **2a**·**3**.

Overall, the inclusion complexations of diquat (**3**) by crown ethers and cryptands involve enclosure of the guest in such a way that charge transfer interactions are allowed, augmenting host–guest hydrogen bonding. This involves folding into 'taco-complexes' for smaller crown ethers,[13a,13b] while for the larger crown ether **2b**[13e] and its *para*-analog[13f] folding is not observed. The structures of cryptands **4** and a dibenzo-30-crown-10-based analog[13c] are pre-organized in taco-like conformations that facilitate π-stacking.

2.6. Electrospray ionization mass spectrometric characterization of diquat complexes

Solutions of cryptands **4** and **5** and crown ether **2a** with diquat **3** in 4:1 acetonitrile/chloroform were characterized by electrospray ionization mass spectrometry (Fig. 8 and Table 2). For all seven diquat complexes, two relevant peaks, $[\mathbf{Host}\cdot\mathbf{3}-\mathrm{PF_6}]^+$ and $[\mathbf{Host}\cdot\mathbf{3}-2\mathrm{PF_6}]^{2+}$, were found. Interestingly for all of them except the complexes between **4b** and **3** and between **4c** and **3**, a peak, $[\mathbf{Host}_2\cdot\mathbf{3}-2\mathrm{PF_6}]^{2+}$, appears to be due to the [3]complex $\mathbf{Host}_2\cdot\mathbf{3}$; this is noteworthy because analogous cryptand/paraquat [3]complexes $\mathbf{4a}_2\cdot\mathbf{1}$ and $\mathbf{5}_2\cdot\mathbf{1}$ have been isolated and characterized by X-ray crystallography.[4f]

3. Conclusions

In summary, seven diquat-based inclusion [2]complexes were studied by proton NMR spectroscopy, electrospray ionization mass spectrometry, and X-ray analysis. Bis(*m*-phenylene)-32-crown-10-based cryptands **4** have been proved to be able to complex diquat much more strongly than bis(*m*-phenylene)-32-crown-10 itself (**2b**) and one containing a pyridyl moiety (**4b**) has one of the highest K_a values reported to date. These hosts form 1:1 complexes with diquat in solution and the solid state. It was found that the improved binding from bis(*m*-phenylene)-32-crown-10 (**2b**) to bis(5-hydroxymethyl-1,3-phenylene)-32-crown-10 (**2a**) was due to the formation of a supramolecular cryptand structure by chelation of the two terminal OH moieties of diol **2a** with a water molecule as a hydrogen-bonding bridge. This efficient cryptand/diquat recognition motif will be used in the preparation of other supramolecular systems. We are working on this project now.

4. Experimental section

4.1. Complexation studies by proton NMR

All solutions were prepared as follows. Precisely weighed amounts of dried hosts and guests were added into separate screw cap vials. The solvent was added with to-deliver volumetric pipettes. Then specific volumes of each fresh solution were mixed to yield the desired concentrations. For example, in order to make three solutions, 0.500 mM **4e**/1.00 mM **3**, 0.500 mM **4e**/3.00 mM **3**, and 0.500 mM **4e**/5.00 mM **3**, a 1.00 mM solution of **4e** was made first by adding 5.00 mL acetone-d_6 with a 5.00 mL to-deliver pipette into a screw cap vial containing 3.35 mg (0.00500 mmol) of **4**. Then 0.300 mL of this solution was added with a 0.300 mL to-deliver pipette to three vials that contained 0.300 mL of 2.00 mM, 0.300 mL of 6.00 mM, and 0.300 mL of 10.0 mM **3** separately. ^{1}H NMR data were collected on a temperature-controlled spectrometer. Acetone-d_6 was chosen as the NMR solvent because all compounds used here have relatively good solubilities in it. Error bars were calculated based on a 0.05 mg deviation in weight, a 0.001 ppm deviation in chemical shift on proton NMR spectra, and a ±2% deviation in fractional complexation (Δ/Δ_0). Standard errors in both the intercept and slope coefficients based on regression were used to determine errors in association constants.

4.1.1. Crystal data of 3. Plate, colorless, 0.065×0.172×0.176 mm^3, $C_{12}H_{12}F_{12}N_2P_2$, FW 474.18, monoclinic, space group $P2_1$, a=6.3160(12), b=14.707(3), c=9.0800(16) Å, β=104.176(16)°, V=817.8(3) Å^3, Z=2, D_c=1.926 g cm^{-3}, T=100 K, μ=3.710 mm^{-1}, 3224 measured reflections, 2698 independent reflections [R(int)=0.0524], 254 parameters,

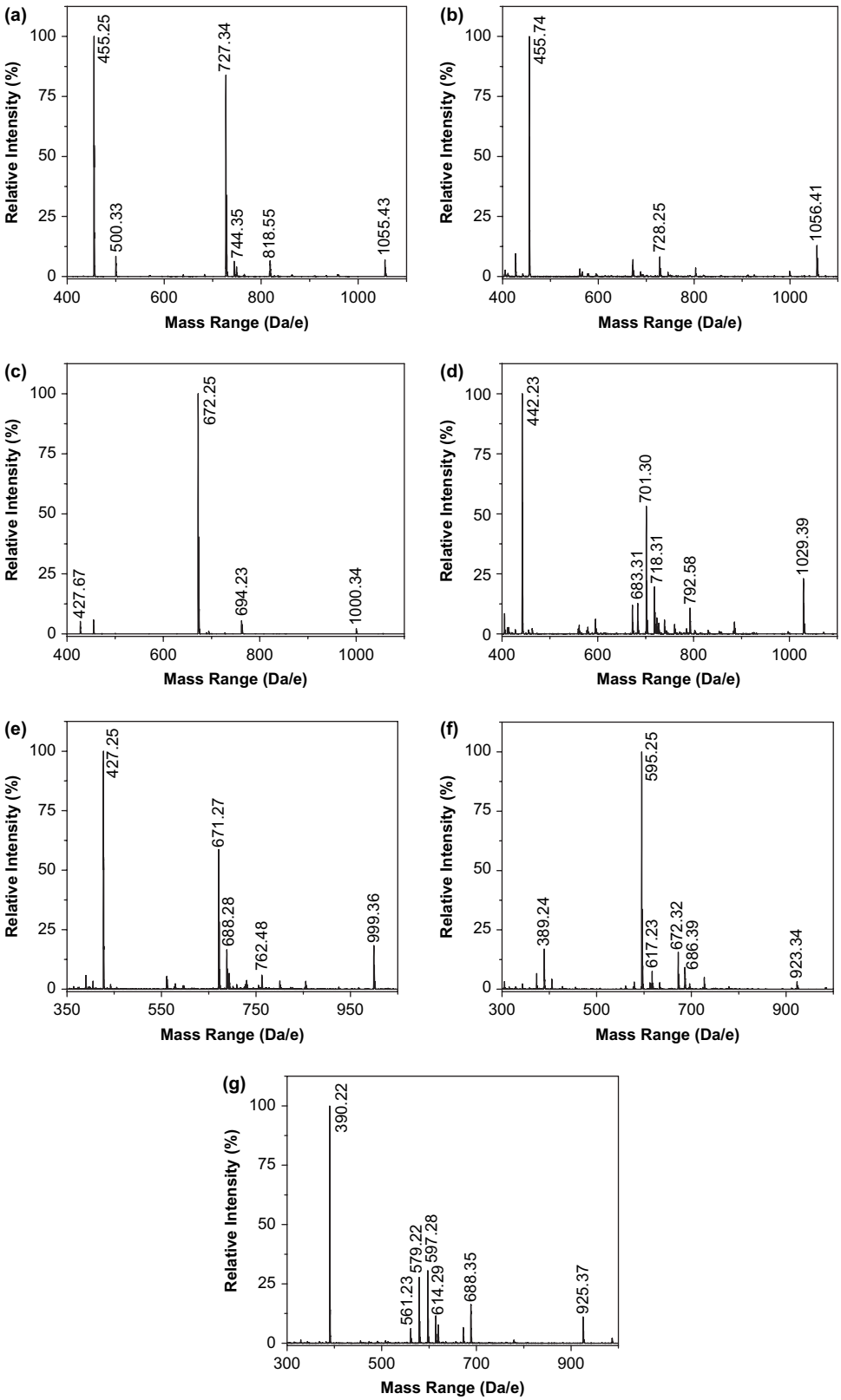

Figure 8. Electrospray mass spectra of solutions of **4a** and **3** (a), **4b** and **3** (b), **4c** and **3** (c), **4d** and **3** (d), **4e** and **3** (e), **5** and **3** (f), and **2a** and **3** (g) in a mixture of acetonitrile and chloroform (4:1). Assignments of main peaks: (a) *m/z* 1055.43 [**4a**·**3**−PF_6]$^+$, 818.55 [**4a**$_2$·**3**−2PF_6]$^{2+}$, 744.35 [**4a**+H_2O]$^+$, 727.34 [**4a**+H]$^+$, 500.33 [**4a**$_2$·**3**−$CH_2CH_2(OCH_2CH_2)_3O$−2PF_6+K]$^{3+}$, and 455.25 [**4a**·**3**–2PF_6]$^{2+}$; (b) *m/z* 1056.41 [**4b**·**3**−PF_6]$^+$, 728.25 [**4b**+H]$^+$, and 455.74 [**4b**·**3**−2PF_6]$^{2+}$; (c) *m/z* 1000.34 [**4c**·**3**−PF_6]$^+$, 694.23 [**4c**+Na]$^+$, 672.25 [**4c**+H]$^+$, and 427.67 [**4c**·**3**–2PF_6]$^{2+}$; (d) *m/z* 1029.39 [**4d**·**3**−PF_6]$^+$, 792.58 [**4d**$_2$·**3**–2PF_6]$^{2+}$, 718.31 [**4d**+H_2O]$^+$, 701.30 [**4d**+H]$^+$, 683.31 [**4d**−OH]$^+$, and 442.23 [**4d**·**3**–2PF_6]$^{2+}$; (e) *m/z* 999.36 [**4e**·**3**−PF_6]$^+$, 762.48 [**4e**$_2$·**3**–2PF_6]$^{2+}$, 688.28 [**4e**+H_2O]$^+$, 671.27 [**4e**+H]$^+$, and 427.25 [**4e**·**3**−2PF_6]$^{2+}$; (f) *m/z* 923.34 [**5**·**3**−PF_6]$^+$, 686.39 [**5**$_2$·**3**−2PF_6]$^{2+}$, 672.32 [**5**$_2$·**3**−2PF_6−CH_2CH_2]$^{2+}$, 617.23 [**5**+Na]$^+$, 595.25 [**5**+H]$^+$, and 389.24 [**5**·**3**−2PF_6]$^{2+}$; (g) *m/z* 925.37 [**2a**·**3**−PF_6]$^+$, 688.35 [**2a**$_2$·**3**−2PF_6]$^{2+}$, 614.29 [**2a**+H_2O]$^+$, 597.28 [**2a**+H]$^+$, 579.22 [**2a**−OH]$^+$, 561.23 [**2a**−OH−H_2O]$^+$, and 390.22 [**2a**·**3**–2PF_6]$^{2+}$.

Table 2. Observed mass/charge ratios for cryptand/diquat and crown ether/diquat complexes in $CH_3CN/CHCl_3$ (4:1) by electrospray ionization mass spectrometry

Host	$[\mathbf{Host}\cdot\mathbf{3}-PF_6]^+$	$[\mathbf{Host}\cdot\mathbf{3}-2PF_6]^{2+}$	$[\mathbf{Host}_2\cdot\mathbf{3}-2PF_6]^{2+}$
4a[a]	1055.43 (6.9%)	455.25 (100%)	818.55 (6.5%)
4b	1056.41 (13.0%)	455.74 (100%)	
4c[b]	1000.34 (3%)	427.67 (6%)	
4d	1029.39 (22%)	442.23 (100%)	792.58 (11%)
4e	999.36 (18%)	427.25 (100%)	762.48 (6%)
5[c,d]	923.34 (3%)	389.24 (17%)	686.39 (9%)
2a	925.37 (11%)	390.22 (100%)	688.35 (16%)

[a] Also found for $\mathbf{4a}_2\cdot\mathbf{3}$: *m/z* 500.33 $[\mathbf{4a}_2\cdot\mathbf{3}-CH_2CH_2(OCH_2CH_2)_3O-2PF_6+K]^{3+}$ (8.4%).
[b] The base peak was at *m/z* 672.25, corresponding to $[\mathbf{4c}+H]^+$.
[c] Also found for $\mathbf{5}_2\cdot\mathbf{3}$: *m/z* 672.32 $[\mathbf{5}_2\cdot\mathbf{3}-2PF_6-CH_2CH_2]^{2+}$ (8.4%).
[d] The base peak was at *m/z* 595.25, corresponding to $[\mathbf{5}+H]^+$.

$F(000)=472$, $R_1=0.0436$, $wR_2=0.1151$ (all data), $R_1=0.0433$, $wR_2=0.1147$ [$I>2\sigma(I)$], and goodness-of-fit (F^2)=1.139. The asymmetric unit of the structure comprises one crystallographically independent salt. The final refinement model involved anisotropic displacement parameters for non-hydrogen atoms and a riding model for all hydrogen atoms. The Flack parameter suggested racemic twinning, which refined to relative occupancies of 68.6% and 31.4%. Crystallographic data (excluding structure factors) for the structures in this paper have been deposited with the Cambridge Crystallographic data Center as supplementary publication numbers CCDC 244377 (**3**), 294375 (**4a·3**), 627713 (**5·3**), 627711 (**2a·3**), and 627712 (**2a·3-TFA**). Copies of the data can be obtained, free of charge, on application to CCDC, 12 Union Road, Cambridge CB2 1EZ, UK [fax: +44 (0)1223 336033 or e-mail: deposit@ccdc.cam.ac.uk].

4.1.2. Crystal data of 4a·3. Rod, yellow, 0.270×0.154×0.078 mm^3, $C_{54}H_{80}F_{12}N_2O_{18}P_2$, FW 1335.14, orthorhombic, space group $Pna2_1$, $a=24.869(2)$, $b=22.922(2)$, $c=10.8407(13)$ Å, $\alpha=\beta=\gamma=90°$, $V=6179.7(11)$ Å^3, $Z=4$, $D_c=1.435$ g cm^{-3}, $T=100$ K, $\mu=1.77$ cm^{-1}, 38,121 measured reflections, 11,848 independent reflections [R(int)=0.0587], 805 parameters, $F(000)=2800$, $R_1=0.0744$, $wR_2=0.1008$ (all data), $R_1=0.0531$, $wR_2=0.0919$ [$I>2\sigma(I)$], maximum residual density 0.351 eÅ^{-3}, and goodness-of-fit (F^2)=1.046. The asymmetric unit of the structure comprises one host–guest complex and two acetone molecules. The final refinement involved anisotropic displacement parameters for non-hydrogen atoms and a riding model for all hydrogen atoms.

4.1.3. Crystal data of 5·3. Plate, yellow, 0.39×0.22×0.026 mm^3, $C_{91.57}H_{123.53}F_{24}N_4O_{26.72}P_4$, FW 2287.65, triclinic, space group P-1, $a=16.5814(19)$, $b=18.919(3)$, $c=19.827(2)$ Å, $\alpha=89.261(12)°$, $\beta=66.455(11)°$, $\gamma=66.741(14)°$, $V=5160.6(12)$ Å^3, $Z=2$, $D_c=1.472$ g cm^{-3}, $T=100$ K, $\mu=1.92$ cm^{-1}, 24,878 measured reflections, 18,072 independent reflections [R(int)=0.0395], 1380 parameters, $F(000)=2381$, $R_1=0.1463$, $wR_2=0.2045$ (all data), $R_1=0.0828$, $wR_2=0.1683$ [$I>2\sigma(I)$], maximum residual density 0.762 eÅ^{-3}, and goodness-of-fit (F^2)=1.130. The asymmetric unit of the structure comprises two host–guest complexes, 2.5222 acetone molecules, and 0.198 water molecule. There were two solvent regions in the asymmetric unit. One region contained a single relatively ordered acetone molecule. The other solvent region clearly exhibited disorder, which was modeled as one fully occupied acetone molecule and one acetone that refined to 52.2% occupancy. Residual electron density approximately 2.6 Å from O6 was modeled as the oxygen of a partially occupied water molecule, which refined to 19.8% occupancy. The final refinement model involved anisotropic displacement parameters for non-hydrogen atoms and a riding model for all hydrogen atoms. Hydrogen atoms of the water were not included in the final refinement.

4.1.4. Crystal data of 2a·3. Block, orange, 0.23×0.16×0.13 mm^3, $C_{117}H_{168}F_{24}N_4O_{40}P_4$, FW 2850.43, monoclinic, space group $P2_1/n$, $a=15.450(3)$, $b=20.768(4)$, $c=20.626(5)$ Å, $\beta=102.825(19)°$, $V=6453(2)$ Å^3, $Z=4$, $D_c=1.467$ g cm^{-3}, $T=100$ K, $\mu=1.77$ cm^{-1}, 41,239 measured reflections, 11,449 independent reflections [R(int)=0.0719], 890 parameters, $F(000)=2988$, $R_1=0.1401$, $wR_2=0.1678$ (all data), $R_1=0.0615$, $wR_2=0.1522$ [$I>2\sigma(I)$], max. residual density 1.032 eÅ^{-3}, and goodness-of-fit (F^2)=0.829. The asymmetric unit of the structure comprises 1.5 crown ether molecules, 1 diquat derivative, 0.5 acetone molecule, and 1.5 water molecules. Upon identifying the host and guest compounds, residual electron density suggested the presence of disorder on one of the crown ethers and the presence of solvent molecules. The alcohol oxygen of one crown ether was modeled as 2-position disorder with relative occupancies of 0.502(6) and 0.498(6) for O11A and O11B, respectively. In addition, two water molecules were assigned based on the residual electron density map. O19 was modeled as fully occupied. O20 could not be fully occupied because it was 2.0 Å from O11A; thus the occupancy was fixed to the same value as O11B (i.e. 0.498(6)). The hydrogen atoms on the water molecules could not be located from the residual electron density map and were not included in the model. A cluster of electron density at the inversion center relating the half-crown ether was modeled as a disordered acetone molecule, with the relative occupancies of the two conformations constrained to 0.5 by symmetry. The final refinement model involved anisotropic displacement parameters for non-hydrogen atoms and a riding model for all hydrogen atoms.

4.1.5. Crystal data of 2a·3-TFA. Plate, yellow, 0.143×0.132×0.034 mm^3, $C_{46}H_{58}F_6N_2O_{17}$, FW 1024.94, monoclinic, space group Pn, $a=11.2302(13)$, $b=9.7297(11)$, $c=21.768(2)$ Å, $\beta=97.322(9)°$, $V=2359.1(5)$ Å^3, $Z=2$, $D_c=1.443$ g cm^{-3}, $T=100$ K, $\mu=1.24$ cm^{-1}, 10,773 measured reflections, 4176 independent reflections [R(int)=0.0391], 650 parameters, $F(000)=1076$, $R_1=0.0684$, $wR_2=0.0906$ (all data), $R_1=0.0503$, $wR_2=0.0829$ [$I>2\sigma(I)$], max. residual density 0.0312 eÅ^{-3}, and goodness-of-fit (F^2)=1.053. The asymmetric unit of the structure comprises one host–guest complex and a water molecule. The final refinement model involved anisotropic displacement parameters for all non-hydrogen atoms and a riding model for all hydrogen atoms, except those of the water. The hydrogen atoms of the water molecule were located in the residual electron density map and restrained to 0.84 Å.

Acknowledgements

This research was supported by the National Science Foundation (DMR0097126) and the American Chemical Society

Petroleum Research Fund (40223-AC7). We also thank NSF (Grant CHE-0131128) for funding of the purchase of the Oxford Diffraction Xcalibur2 single crystal diffractometer. F.H. thanks the National Natural Science Foundation of China (20604020) and Zhejiang Province (2006R10003) for financial support.

Supplementary data

Supplementary data associated with this article can be found in the online version, at doi:10.1016/j.tet.2007.01.042.

References and notes

1. Badjic, J. D.; Balzani, V.; Credi, A.; Silvi, S.; Stoddart, J. F. *Science* **2004**, *303*, 1845–1849; Hernandez, J. V.; Kay, E. R.; Leigh, D. A. *Science* **2004**, *306*, 1532–1537; Huang, F.; Gibson, H. W. *J. Am. Chem. Soc.* **2004**, *126*, 14738–14739; Huang, F.; Nagvekar, D. S.; Slebodnick, C.; Gibson, H. W. *J. Am. Chem. Soc.* **2005**, *127*, 484–485; Fuller, A.-M. L.; Leigh, D. A.; Lusby, P. J.; Slawin, A. M. Z.; Walker, D. B. *J. Am. Chem. Soc.* **2005**, *127*, 12612–12619; Versteegen, R. M.; Van Beek, D. J. M.; Sijbesma, R. P.; Vlassopoulos, D.; Fytas, G.; Meijer, E. W. *J. Am. Chem. Soc.* **2005**, *127*, 13862–13868; Pittelkow, M.; Nielsen, C. B.; Broeren, M. A. C.; van Dongen, J. L. J.; van Genderen, M. H. P.; Meijer, E. W.; Christensen, J. B. *Chem.—Eur. J.* **2005**, *11*, 5126–5135; Huang, F.; Gantzel, P.; Nagvekar, D. S.; Rheingold, A. L.; Gibson, H. W. *Tetrahedron Lett.* **2006**, *47*, 7841–7844; Kay, E. R.; Leigh, D. A. *Nature* **2006**, *440*, 286–287.
2. (a) The International Union of Pure and Applied Chemistry defines a cryptand as follows: “a molecular entity comprising a cyclic or polycyclic assembly of binding sites that contains three or more binding sites held together by covalent bonds, and which defines a molecular cavity in such a way as to bind (and thus ‘hide’ in the cavity) another molecular entity, the guest (a cation, an anion or a neutral species), more strongly than do the separate parts of the assembly (at the same total concentration of binding sites). — The term is usually restricted to bicyclic or oligocyclic molecular entities”; (b) Simmons, H. E.; Park, C. H. *J. Am. Chem. Soc.* **1968**, *90*, 2428–2429; 2429–2431; 2431–2432; (c) Reviews: Dietrich, B. *Comprehensive Supramolecular Chemistry*; Lehn, J.-M., Atwood, J. L., Davies, J. E. D., McNicol, D. D., Vogtle, F., Eds.; Pergamon: Oxford, 1996; Vol. 1, pp 153–211; Lucht, B. L.; Collum, D. B. *Acc. Chem. Res.* **1999**, *32*, 1035–1042; Reed, C. A.; Bolskar, R. D. *Chem. Rev.* **2000**, *100*, 1075–1120; Kaes, C.; Katz, A.; Hosseini, M. W. *Chem. Rev.* **2000**, *100*, 3553–3590.
3. Supramolecular cryptands have been referred to as ‘pseudo-cryptands’. For the first such reference, see: Nabeshima, T.; Inaba, T.; Sagae, T.; Furukawa, N. *Tetrahedron Lett.* **1990**, *31*, 3919–3922; For examples of recent references, see: (a) Romain, H.; Florence, D.; Alain, M. *Chemistry* **2002**, *8*, 2438–2445; (b) Nabeshima, T.; Yoshihira, Y.; Saiki, T.; Akine, S.; Horn, E. *J. Am. Chem. Soc.* **2003**, *125*, 28–29; For a review, see: Nabeshima, T.; Akine, S.; Saiki, T. *Rev. Heteroatom Chem.* **2000**, *22*, 219–239.
4. (a) Rowan, A. E.; Aarts, P. P. M.; Koutstaal, K. W. M. *Chem. Commun.* **1998**, 611–612; (b) Gunter, M. J.; Jeynes, T. P.; Johnston, M. R.; Turner, P.; Chen, Z. *J. Chem. Soc., Perkin Trans. 1* **1998**, 1945–1957; (c) Elemans, J. A. A. W.; Claase, M. B.; Aarts, P. P. M.; Rowan, A. E.; Schenning, A. P. H. J.; Nolte, R. J. M. *J. Org. Chem.* **1999**, *64*, 7009–7016; (d) Bryant, W. S.; Jones, J. W.; Mason, P. E.; Guzei, I. A.; Rheingold, A. L.; Nagvekar, D. S.; Gibson, H. W. *Org. Lett.* **1999**, *1*, 1001–1004; (e) Huang, F.; Fronczek, F. R.; Gibson, H. W. *J. Am. Chem. Soc.* **2003**, *125*, 9272–9273; (f) Huang, F.; Gibson, H. W.; Bryant, W. S.; Nagvekar, D. S.; Fronczek, F. R. *J. Am. Chem. Soc.* **2003**, *125*, 9367–9371; (g) Huang, F.; Zhou, L.; Jones, J. W.; Gibson, H. W.; Ashraf-Khorassani, M. *Chem. Commun.* **2004**, 2670–2671; (h) Huang, F.; Switek, K. A.; Zakharov, L. N.; Fronczek, F. R.; Slebodnick, C.; Lam, M.; Golen, J. A.; Bryant, W. S.; Mason, P.; Rheingold, A. L.; Ashraf-Khorassani, M.; Gibson, H. W. *J. Org. Chem.* **2005**, *70*, 3231–3241.
5. (a) Huang, F.; Zakharov, L. N.; Rheingold, A. L.; Jones, J. W.; Gibson, H. W. *Chem. Commun.* **2003**, 2122–2123; (b) Huang, F.; Slebodnick, C.; Rheingold, A. L.; Switek, K. A.; Gibson, H. W. *Tetrahedron* **2005**, *61*, 10242–10253; (c) Huang, F.; Fronczek, F. R.; Ashraf-Khorassani, M.; Gibson, H. W. *Tetrahedron Lett.* **2005**, *46*, 6765–6769.
6. (a) Jones, J. W.; Zakharov, L. N.; Rheingold, A. L.; Gibson, H. W. *J. Am. Chem. Soc.* **2002**, *124*, 13378–13379; (b) Huang, F.; Guzei, I. A.; Jones, J. W.; Gibson, H. W. *Chem. Commun.* **2005**, 1693–1695.
7. Cram, D. J. *Science* **1988**, *240*, 760–767.
8. Reetz, M. T.; Niemeyer, C. M.; Harms, K. *Angew. Chem., Int. Ed. Engl.* **1991**, *30*, 1472–1474; Reetz, M. T.; Niemeyer, C. M.; Harms, K. *Angew. Chem., Int. Ed. Engl.* **1991**, *30*, 1474–1476; Reetz, M. T.; Niemeyer, C. M.; Hermes, M.; Goddard, R. *Angew. Chem., Int. Ed. Engl.* **1992**, *31*, 1017–1019; Reetz, M. T.; Huff, J.; Goddard, R. *Tetrahedron Lett.* **1994**, *35*, 2521–2524.
9. Niikura, K.; Bisson, A. P.; Anslyn, E. V. *J. Chem. Soc., Perkin Trans. 2* **1999**, 1111–1114.
10. Hashizume, M.; Tobey, S.; Lynch, V. M.; Anslyn, E. V. *Supramol. Chem.* **2002**, *14*, 511–517.
11. Mahoney, J. M.; Beatty, A. M.; Smith, B. D. *J. Am. Chem. Soc.* **2001**, *123*, 5847–5848; Mahoney, J. M.; Stucker, K. A.; Jiang, H.; Carmichael, I.; Brinkmann, N. R.; Beatty, A. M.; Noll, B. C.; Smith, B. D. *J. Am. Chem. Soc.* **2005**, *127*, 2922–2928.
12. Fuke, C. *Drugs and Poisons in Humans: A Handbook of Practical Analysis*; Suzuki, O., Watanabe, K., Eds.; Springer: New York, NY, 2005; pp 571–580; Xie, L.; Thrippleton, K.; Irwin, M. A.; Siemering, G. S.; Mekebri, A.; Crane, D.; Berry, K.; Schlenk, D. *Toxicol. Sci.* **2005**, *87*, 391–398; Aramendia, M. A.; Borau, V.; Lafont, F.; Marinas, A.; Marinas, J. M.; Moreno, J. M.; Porras, J. M.; Urbano, F. J. *Food Chem.* **2006**, *97*, 181–188.
13. (a) Colquhoun, H. M.; Goodings, E. P.; Maud, J. M.; Stoddart, J. F.; Williams, D. J.; Wolstenholme, J. B. *J. Chem. Soc., Chem. Commun.* **1983**, 1140–1142; (b) Colquhoun, H. M.; Goodings, E. P.; Maud, J. M.; Stoddart, J. F.; Wolstenholme, J. B.; Williams, D. J. *J. Chem. Soc., Perkin Trans. 2* **1985**, 607–624; (c) Allwood, B. L.; Kohnke, F. H.; Slawin, A. M. Z.; Stoddart, J. F.; Williams, D. J. *J. Chem. Soc., Chem. Commun.* **1985**, 311–314; (d) Kohnke, F. H.; Stoddart, J. F. *J. Chem. Soc., Chem. Commun.* **1985**, 314–317; (e) Allwood, B. L.; Shahriari-Zavareh, H.; Stoddart, J. F.; Williams, D. J. *J. Chem. Soc., Chem. Commun.* **1987**, 1058–1061; (f) Allwood, B. L.; Spencer, N.; Shahriari-Zavareh, H.; Stoddart, J. F.; Williams, D. J. *J. Chem. Soc., Chem. Commun.* **1987**, 1061–1064; (g) Anelli, P. L.; Spencer, N.; Stoddart, J. F. *Tetrahedron Lett.* **1988**, *29*, 1569–1572; (h) Anelli, P. L.;

Slawin, A. M. Z.; Stoddart, J. F.; Williams, D. J. *Tetrahedron Lett.* **1988**, *29*, 1573–1574; (i) Gunter, M. J.; Johnston, M. R. *Tetrahedron Lett.* **1992**, *33*, 1771–1774; (j) Gunter, M. J.; Jeynes, T. P.; Johnston, M. R.; Turner, P.; Chen, Z. *J. Chem. Soc., Perkin Trans. 1* **1998**, 1945–1958; (k) Huang, F.; Slebodnick, C.; Switek, K. A.; Gibson, H. W. *Chem. Commun.* **2006**, 1929–1931.

14. Job, P. *Ann. Chim.* **1928**, *9*, 113–203.
15. ^{1}H NMR characterizations were done on solutions with constant $[\mathbf{4a}]_0$ and varied $[\mathbf{3}]_0$. Based on these NMR data, Δ_0, the difference in δ values for H_1 of **4a** in the uncomplexed and fully complexed species, was determined as the *y*-intercept of a plot of $\Delta=\delta-\delta_u$ versus $1/[\mathbf{3}]_0$ in the high initial concentration range of **3**; Δ_0=0.448 ppm. Then $p=\Delta/\Delta_0$; Δ=observed chemical shift change relative to uncomplexed species. The value of the association constant ($K_{a,\mathbf{4a}\cdot\mathbf{3}}$) of **4a**·**3** was calculated in two ways. The first way was by using the Benesi–Hildebrand method (Benesi, H. A.; Hildebrand, J. H. *J. Am. Chem. Soc.* **1949**, *71*, 2703). Eight data points ranging from p=0.313 to 0.993 were used. The resultant $K_{a,\mathbf{4a}\cdot\mathbf{3}}$ value is 2.0 ($\pm$0.2)$\times10^4$ M^{-1}, as previously reported in the short communication of this full article.[13k] The second way was by using the average p value in several solutions with 1 mM host and guest. Then the $K_{a,\mathbf{4a}\cdot\mathbf{3}}$ value was calculated from $K_{a,\mathbf{4a}\cdot\mathbf{3}}=p/\{(1-p)([\mathbf{3}]_0-p[\mathbf{4a}]_0)\}$ to be 4.3 ($\pm$0.4)$\times10^4$ M^{-1}, which is reported in this full article. All K_a values, except the one for complex **4b**·**3**, in Table 1 were calculated in this way. The concentrations of 1 mM host and guest were chosen for comparison. It was found that for the systems reported in this paper, K_a values are not concentration dependent as we found in some other systems.[16] Concentration dependence of K_a calculated in this manner results when the complexes are not ion paired, but the guest salts are ion paired. In such cases, more extensive studies are required to determine the dissociation constant for the ion pair and the binding constant for the cationic guest with the host.[16] The calculated Δ_0 and p values in 1 mM host and guest acetone solutions for **4a**·**3**, **4c**·**3**, **4d**·**3**, **4e**·**3**, **5**·**3**, and **2a**·**3** are 0.448 ppm and 0.859, 0.337 ppm and 0.694, 0.112 ppm and 0.473, 0.358 ppm and 0.369, 0.211 ppm and 0.275, and 0.202 ppm and 0.553, respectively. The chemical shift changes for H_1 of **4a**, **4c** and **4e**, H_9 of **4d**, H_7 of **5**, and H_8 of **2a** were used in these association constant calculations.
16. Jones, J. W.; Gibson, H. W. *J. Am. Chem. Soc.* **2003**, *125*, 7001–7004; Huang, F.; Jones, J. W.; Slebodnick, C.; Gibson, H. W. *J. Am. Chem. Soc.* **2003**, *125*, 14458–14464; Gibson, H. W.; Wang, H.; Bonrad, K.; Jones, J. W.; Slebodnick, C.; Habenicht, B.; Lobue, P. *Org. Biomol. Chem.* **2005**, *3*, 2114–2121.
17. Heath, R. E.; Dykes, G. M.; Fish, H.; Smith, D. K. *Chem.—Eur. J.* **2003**, *9*, 850–855.
18. In a 0.670 mM equimolar acetone-d_6 solution of reference host **4a**, **4b**, and guest **3**, the concentration of complexed **4a**, $[\mathbf{4a}]_c$, was 0.174 mM. $K_{a,\mathbf{4b}\cdot\mathbf{3}}$ was thus determined to be 3.3 ($\pm$0.7)$\times10^5$ M^{-1}. The error is based on errors of $[\mathbf{4a}]_c$ and $K_{a,\mathbf{4a}\cdot\mathbf{3}}$, 4.3 ($\pm$0.4)$\times10^4$ M^{-1}.
19. Hansch, C.; Leo, A.; Taft, R. W. *Chem. Rev.* **1991**, *91*, 165–195.